Kinetic bottleneck to the self-organization of bidisperse hard disk monolayers formed by random sequential adsorption

R. Christopher Doty, Roger T. Bonnecaze,*,† and Brian A. Korgel*,‡
Department of Chemical Engineering, Texas Materials Institute, Center for Nano- and Molecular Science and Technology, The University of Texas, Austin, Texas 78712-1062
(Received 15 January 2002; published 19 June 2002)

We study the self-organization of bidisperse mixtures of hard spheres in two dimensions by simulating random sequential adsorption (RSA) of tethered hard disks that undergo limited Monte Carlo surface diffusion. The tethers place a control on the local entropy of the disks by constraining their movement within a specified distance from their original adsorption positions. By tuning the tether length, from zero (the pure RSA process) to infinity (near-equilibrium conditions), the kinetic pathway to monolayer formation can be varied. Previously [J. J. Gray *et al.*, Phys. Rev. Lett. **85**, 4430 (2000); Langmuir **17**, 2317 (2001)], we generated nonequilibrium phase diagrams for size-monodisperse and size-polydisperse hard disks as a function of surface coverage, size distribution, and tether length to reveal the occurrence of hexagonal close-packed, hexatic, and disordered phases. Bidisperse hard disks potentially offer increasingly diverse phase diagrams, with the possible occurrence of spatially and compositionally organized superlattices. Geometric packing calculations anticipate the formation of close-packed lattices in two dimensions for particle size ratios $\sigma = R_S/R_L = 0.53$, 0.414, and 0.155. The simulations of these systems presented here, however, reveal that RSA kinetics frustrate superlattice ordering, even for infinite tethers. The calculated jamming limits fall well below the minimum surface coverages necessary for stable ordering, as determined by melting simulations.

DOI: 10.1103/PhysRevE.65.061503 PACS number(s): 61.43.Bn, 81.07.−b

INTRODUCTION

Particles that experience hard sphere interactions with interparticle potential Φ, defined as a function of the center-to-center interparticle separation r, and the particle radius R, where

$$\Phi = \begin{cases} \infty & \text{if } r \leqslant 2R, \\ 0 & \text{if } r > 2R, \end{cases} \tag{1}$$

represent an important model for understanding fluid-solid phase behavior [1]. Understandably, hard spheres cannot give rise to gas-liquid phase coexistence, as there is no cohesive force between particles; however, hard spheres do in fact give rise to a first order fluid-solid phase transition in three dimensions (3D) [2]. This disorder-order transition arises solely from the entropy *increase* gained upon organizing into a lattice at high packing fractions. The system loses configurational entropy, but gains significant free volume entropy by ordering. Consider, for example, that the maximum packing of a face-centered-cubic lattice in 3D is 0.74 as opposed to ~0.64 for the random close-packed structure [3]—one might view the ordering transition as a disorder-avoiding transition. The phase behavior for bidisperse systems of hard spheres is significantly more complex than for the monodisperse system. One must consider the size ratio, $\sigma = R_S/R_L$, between the large R_L and small R_S particles and the number fractions or volume fractions of each size, namely, n_S, n_L, ϕ_S, and ϕ_L. The fact that binary solids of large and small particles can form with various stoichiometries L_mS_n complicates matters significantly. In terms of identifying stable lattices of bidisperse hard spheres in three dimensions, both theoretical and experimental efforts have yielded significant results [4–9]. One of the most useful observations from these studies has been the realization that geometric packing calculations provide reasonable predictions of stable L_mS_n phases of hard spheres [8]. This result has broad significance, as real systems with more complicated interparticle interactions can often be mapped effectively onto hard sphere phase diagrams, thus providing insight into the phase behavior of more complex systems [10–12].

In two dimensions, the situation is qualitatively different. Many years ago, Peierls showed that thermal fluctuations disrupt true long range order in 2D systems [13]. Mermin later showed conclusively that true long range order is impossible in 2D; however, these conclusions could not be drawn for hard spheres [14]. Nonetheless, for all practical purposes, translational order does occur in 2D at sufficiently high surface area coverage. The nature of the freezing transition in 2D, however, remains under debate and it is still not known whether the transition is first order [15,16]. Much of the controversy stems from Kosterlitz-Thouless-Halperin-Nelson-Young theory predictions showing that the 2D melting transition is continuous and second order [17–19]. Given the substantial qualitative differences between 2D and 3D phase behavior, it is questionable how meaningful geometric packing calculations will be in providing insight into the existence of stable L_mS_n phases. Regardless, geometric packing considerations have been used to predict a variety of ordered lattices and have been invoked to explain the recent

*Corresponding authors. FAX: (512) 471-7060.
†Electronic address: rtb@che.utexas.edu
‡Electronic address: korgel@mail.che.utexas.edu

observation of 2D ordered superlattices of bidisperse sterically stabilized gold nanocrystals [20,21].

In real materials systems, *both* thermodynamic and kinetic effects constrain the phase behavior. For example, in the case of quasicrystals, geometric packing calculations can provide guidelines for possible structures; however, quasicrystal formation undoubtedly depends intimately on the kinetic path to phase formation [22]. In protein and colloid crystallization, kinetics plays a fundamental role. The use of simulations to gain an understanding of how kinetics affect colloidal assembly is a daunting task due to the extreme computational power required to witness transitions from densely packed metastable states to equilibrium structures [23]. Nonetheless, we recently developed an approach for studying the effect of kinetics on hard sphere phase evolution in 2D [24,25]. The approach is a modification of the random sequential adsorption (RSA) process for building up a monolayer of particles (or hard disks). A control parameter, the tether length L/R_L, is used to tune the system from kinetically limited to near-equilibrium conditions. The tethers control the local entropy of an adsorbed particle after incorporation into the monolayer. Adsorbed disks diffuse freely between adsorption attempts on the surface within the boundaries set by the tether: a tether length of zero represents the pure RSA process [26,27]; whereas, an infinite tether provides near-equilibrium conditions. We found that hard disks order into hexagonal close-packed lattices with relatively short tether lengths, $L/R_L \cong 4$. Furthermore, the ordering transition proceeds from the disordered phase through a *hexatic* phase before organizing with long range translational order. In the range $1 < L/R_L < 4$, the monolayer locks into the hexatic phase—even when the surface coverage jamming limits are greater than those required for crystal formation at the longer tether lengths—and tethers less than one particle radius frustrate organization altogether. Therefore, we naturally considered if bidisperse hard disks with the appropriate σ for ordered L_mS_n lattice formation determined by geometric packing calculations ($\sigma = 0.53$ (LS_2), 0.414 (LS), and 0.155 (LS_2) [20]) would organize during the tethered RSA process. We were particularly curious, given the absence of any simulated (either using computer or experimental models) L_mS_n phases of hard spheres in 2D in the literature [28,29].

EXPERIMENT

The tethered RSA simulations are performed as described in Refs. [24] and [25]. Hard disks are adsorbed to the surface following the standard RSA procedure of attaching particles to random anchor locations in a periodically replicated square and rejecting overlapping particle placements. The system is $50 \times 50 (R_L)^2$, where R_L is the radius of the largest adsorbing particles. Particle adsorption follows one of two routes. In the first, the ratio of the bulk number fractions ($n_{S,\mathrm{bulk}}/n_{L,\mathrm{bulk}}$) is maintained, allowing the fraction of small n_S and large n_L particles on the surface to vary with time. In the second, the ratio of the surface number fractions (n_S/n_L) is maintained. This is accomplished by choosing a particle for adsorption such that its successful attachment to the surface will on average satisfy the number fraction required by the L_mS_n array of interest. Particles diffuse on the surface between adsorption attempts according to a Monte Carlo scheme that adjusts step size to obtain 50% acceptance of moves [30]. The magnitude and direction of each move are selected from two uniform distributions. Moves that place the particle outside the range of the tether or lead to particle overlap are rejected. Two hundred Monte Carlo cycles are completed after every successful adsorption attempt, where a cycle is defined as N successful moves, with N as the current number of particles on the surface. Since most particle adsorption attempts are unsuccessful (10^{-8} success rate at long times), surface diffusion rates far exceed particle addition rates at long times when the important phase behavior and kinetics are observed.

Melting simulations are performed starting with a perfect L_mS_n lattice and allowing particle diffusion to occur according to the Monte Carlo scheme used in the RSA simulations. Simulations were performed for LS and LS_2 lattices comprised of large and small discs with the appropriate size ratios, $\sigma = 0.155$ (LS_2), 0.414 (LS), and 0.53 (LS_2), determined by Likos and Henley [20]. The initial surface coverage was decreased by increasing the interparticle spacing.

Overlap calculations are implemented using a grid of 400 cells to accelerate computation. By dividing the simulation box into cells, only those cells that serve as a destination for particle addition or diffusion need to be investigated for particle overlap. RSA simulations were run for 3–7 days on a SGI or HP Unix workstation. Melting simulation times were highly dependent on the surface coverage, i.e., low surface coverages melted after only a few minutes of simulation time or less than 1000 diffusion attempts, while others remained stable after 24 h of simulation time or diffusion attempts of the order of 10^6.

RESULTS

Ordered L_mS_n structures were not observed for RSA simulations regardless of the size ratio σ or the length of the tether L/R_L. It was essentially impossible to maintain a constant ratio n_S/n_L on the surface (and therefore, to hit the target n_S/n_L) during the course of the RSA simulations when $n_{S,\mathrm{bulk}}/n_{L,\mathrm{bulk}}$ was fixed, as the small particles always enrich the surface at long times (refer to Figs. 1 and 2). The kinetic data from selected simulations are shown in Fig. 3. The kinetic data can be replotted in power law form (generalizing the form observed first by Feder [26] and derived by Swendsen [27]):

$$\theta = \theta_\infty - \alpha \left(\frac{\gamma a}{A} \right)^{-\beta}, \tag{2}$$

where θ is the fractional areal coverage on the surface and γ is the number of adsorption attempts normalized by the area of the simulation cell A, and the disk area a, to obtain the jamming limit coverages θ_∞, and the two kinetic parameters, α and β. Table I shows θ_∞, α, and β, fit to the kinetic data at long times using the Levenberg-Marquardt algorithm. For simulations with the bulk number fraction held constant at

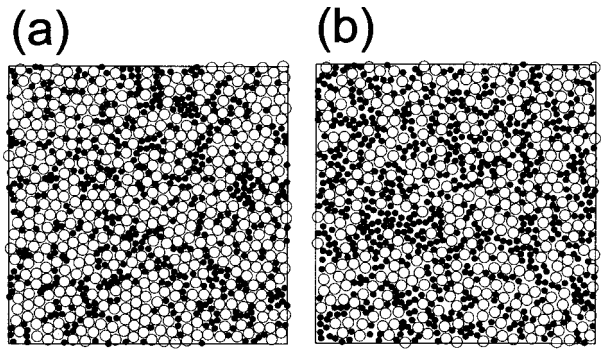

FIG. 1. Tethered RSA simulations. (a) 967 total particles; $\theta = 0.74$, $\sigma = 0.53$, $n_{S,\mathrm{bulk}}/n_{L,\mathrm{bulk}} = 0.04$ (maintained number fraction), $n_S/n_L = 1.2$, $L/R_L = 5$. (b) 1012 total particles; $\theta = 0.66$, $\sigma = 0.53$, $n_{S,\mathrm{bulk}}/n_{L,\mathrm{bulk}} = 2$, $n_S/n_L = 2$ (maintained number fraction), $L/R_L = \infty$.

$n_{S,\mathrm{bulk}}/n_{L,\mathrm{bulk}} = 1/25$ ($L/R_L = 5$), at two different size ratios $R_S/R_L = 0.53$ and $R_S/R_L = 0.414$, $\theta_\infty = 0.91$ and $\theta_\infty = 0.94$, respectively. Note that for $\sigma = 0.53$ and 0.414, the coverages at maximum packing are 0.914 and 0.920, respectively, within the experimental error for θ_∞. The coverage at maximum packing for $\sigma = 0.155$ is 0.95. The kinetic exponent β was found to be 0.11 and 0.12, much lower than $\beta = 0.5$, characteristic of the standard RSA model. It has been proposed that β is related to the degrees of freedom, d, of the system ($\beta \sim 1/d$) [27,31], implying that the tethers and the disk size distribution increase the effective dimensionality of the system. Values of β are similar to those reported in Refs. [24] and [25] for equivalent values of L/R_L, $0.1 < \beta < 0.2$. β appears to be a weak function of $n_{S,\mathrm{bulk}}/n_{L,\mathrm{bulk}}$, while depending sensitively on the polydispersity and tether length. Values for α were determined to be 0.51 and 0.58, slightly higher than the 0.4 determined previously for systems with similar L/R_L [24,25]. The jamming limit coverages are higher for the bidisperse disks studied here than those studied with Gaussian size distributions in Ref. [25]. The greater size difference between large and small particles in the bidisperse distributions provides more free space among the large particles for small particle adsorption to occur, which leads to higher θ_∞.

In order to reach targeted values of n_S/n_L required for $L_m S_n$ ordering, tethered RSA simulations were also performed with fixed n_S/n_L. Ordering of the bidisperse particles still did not occur, even at infinite tether length. Figures 1(b), 2(a), 2(b), and 4 show representative images of the random close-packed structures obtained in these simulations for various size ratios. When n_S/n_L is held constant, the kinetics of monolayer formation are significantly different from those when $n_{S,\mathrm{bulk}}/n_{L,\mathrm{bulk}}$ is held constant (see Fig. 3). For example, θ_∞ varied between 0.71 and 0.73 for various

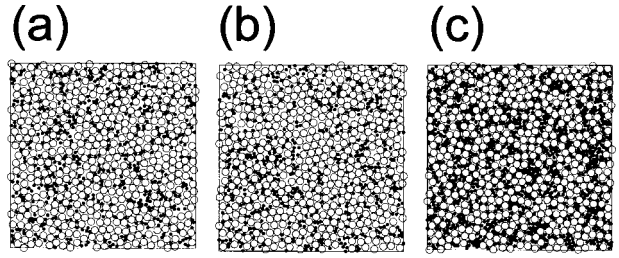

FIG. 2. Tethered RSA simulations. (a) 911 total particles; $\theta = 0.67$, $\sigma = 0.414$, $n_{S,\mathrm{bulk}}/n_{L,\mathrm{bulk}} = 1$, $n_S/n_L = 1$ (maintained number fraction), $L/R_L = \infty$. (b) 931 total particles; $\theta = 0.68$, $\sigma = 0.414$, $n_{S,\mathrm{bulk}}/n_{L,\mathrm{bulk}} = 1$, $n_S/n_L = 1$ (maintained number fraction), $L/R_L = 5$. (c) 1376 total particles; $\theta = 0.75$, $\sigma = 0.414$, $n_{S,\mathrm{bulk}}/n_{L,\mathrm{bulk}} = 0.04$ (maintained number fraction), $n_S/n_L = 2.2$, $L/R_L = 5$.

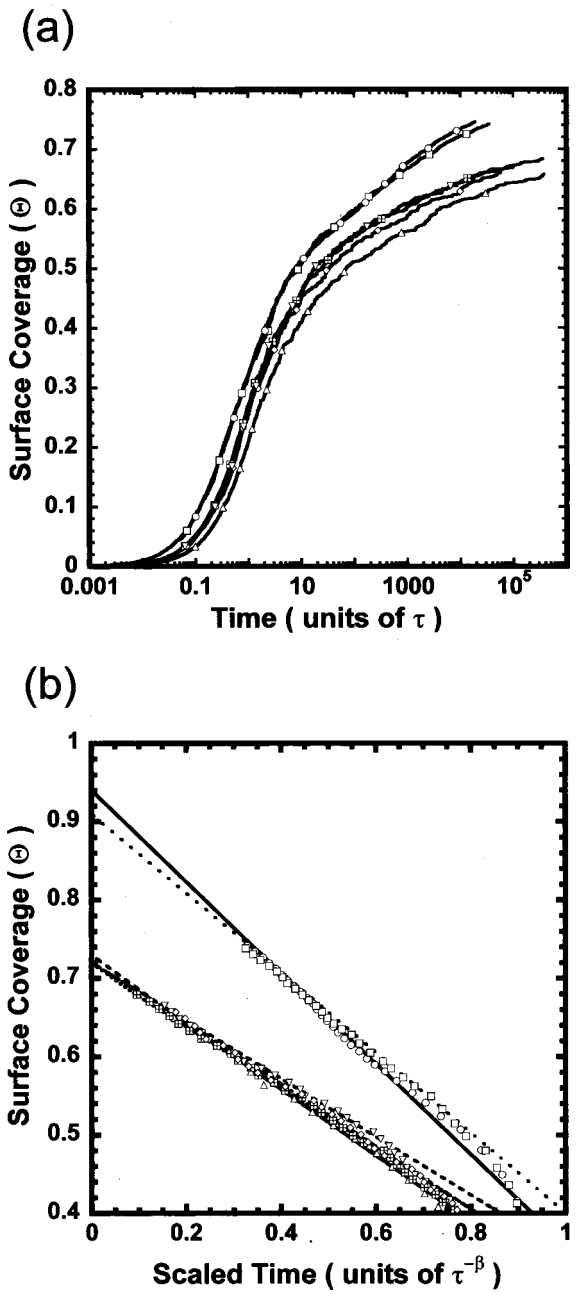

FIG. 3. Kinetic results. (a) Coverage versus time ($\tau = \gamma\alpha/A$) and (b) coverage vs scaled time ($\tau^{-\beta}$) for various tether lengths, size ratios, and surface and bulk concentrations: (△) $\sigma = 0.155$, $n_S/n_L = 2$, $L/R_L = \infty$; (▽) $\sigma = 0.414$, $n_S/n_L = 1$, $L/R_L = \infty$; (⊞) $\sigma = 0.414$, $n_S/n_L = 1$, $L/R_L = 5$; (○) $\sigma = 0.414$, $n_{S,\mathrm{bulk}}/n_{L,\mathrm{bulk}} = 0.04$, $L/R_L = 5$; (◇) $\sigma = 0.53$, $n_S/n_L = 2$, $L/R_L = \infty$; (□) $\sigma = 0.53$, $n_{S,\mathrm{bulk}}/n_{L,\mathrm{bulk}} = 0.04$, $L/R_L = 5$. The lines in (b) correspond to fits from Eq. (2).

TABLE I. Kinetic parameters determined using Eq. (2) from the data shown in Fig. 3.

R_S/R_L	n_S/n_L	L/R_L	θ_∞	α	β
0.155	2	∞	0.73 ± 0.01	0.42 ± 0.001	0.14 ± 0.01
0.53	0.04[a]	5	0.91 ± 0.06	0.51 ± 0.03	0.11 ± 0.03
0.53	2	∞	0.72 ± 0.01	0.40 ± 0.001	0.16 ± 0.01
0.414	0.04[a]	5	0.94 ± 0.04	0.58 ± 0.01	0.12 ± 0.03
0.414	1	5	0.72 ± 0.01	0.39 ± 0.01	0.19 ± 0.02
0.414	1	∞	0.72 ± 0.03	0.37 ± 0.01	0.18 ± 0.05

[a]These are values of $n_{S,\mathrm{bulk}}/n_{L,\mathrm{bulk}}$.

conditions—$\sigma=0.155$, 0.414, and 0.53; $n_S/n_L=2$ and 1; and $L/R_L=5$ and ∞. This is a considerable decrease compared to the situation where only the bulk concentration was specified ($\theta_\infty>0.90$). By specifying the number fraction of small and large disks on the surface, large particles are forced onto the surface with great difficulty at long times. β is slightly higher for the controlled surface concentration case, $0.14<\beta<0.19$ compared to $0.11<\beta<0.12$. Therefore, it would appear that the number of degrees of freedom in the system effectively decreases when the surface concentration is held constant. All the β values are lower than the classical RSA value of 0.5. α values of ≈0.4 are consistent with those determined previously in monodisperse and polydisperse systems with similar tether lengths [24,25]. For monodisperse disks with L/R_L similar to those used in this study, the liquid to hexatic transition takes place at $\theta=0.70$, and a hexatic to crystal transition takes place at $\theta=0.74$. When only $n_{S,\mathrm{bulk}}/n_{L,\mathrm{bulk}}$ is held constant, $\theta>0.74$ at the end of the simulation, however, the monolayer clearly does not exhibit crystalline order [see Figs. 1(a) and 2(c), $\theta=0.742$ and 0.745]. When the surface concentration n_S/n_L is fixed, θ falls well below that necessary for a liquid to hexatic transition, with $\theta=0.661$, 0.670, and 0.684 [see Figs. 1(b), 2(a), and 2(b)].

Melting simulations (or simulations of mechanical stability) were performed to determine the lower bounds on θ for stable LS and LS_2 lattice formation. For $\sigma=0.155$, melting simulations showed that $\theta>0.9$ is necessary to maintain an ordered LS_2 array. This is well above the jamming limit coverage of $\theta_\infty=0.73$. Figure 5 shows the melting of an LS_2 array with $\sigma=0.155$. For $\sigma=0.414$, the surface concentration necessary for ordering into an LS lattice was found to be between 0.78 and 0.81 (see Figs. 6 and 7). This, too, is well above $\theta_\infty=0.72$. For $\sigma=0.53$, the surface concentration for ordering into an LS_2 array was found to fall between 0.78 and 0.82 (see Figs. 8 and 9), well above $\theta_\infty=0.72$. For every size ratio studied, θ_∞ fell far below the values of θ required for mechanical stability. With controlled n_S/n_L, the necessary surface coverage for mechanically stable LS and LS_2 arrays cannot be reached. When the ratio of large and small disks is controlled only in the bulk, higher jamming limits are achieved, but at the expense of small particle enrichment on the surface due to the kinetically preferential adsorption of the small disks at long times. Hence, the surface concentration does not favor LS and LS_2 formation.

Ordered L_mS_n lattices of bidisperse disks in 2D cannot be reached by a tethered RSA process. This result does not necessarily indicate that the L_mS_n phases are not the *equilibrium* phases at high packing fraction. Certainly, the melting simulations revealed that the bidisperse lattices appear to be stable for a small range of dense packing fractions, and perhaps a different path to monolayer formation exists that would allow dense packing fractions with both spatial and compositional order to be reached. However, it is clear from the simulations here that entropy plays a particularly disruptive role during the organization of bidisperse disks in 2D. In the bidisperse case, greater configurational entropy is expected than in the monodisperse case because there are two different types of particles that require not only spatial order, but also *compositional* order. Given that geometric packing

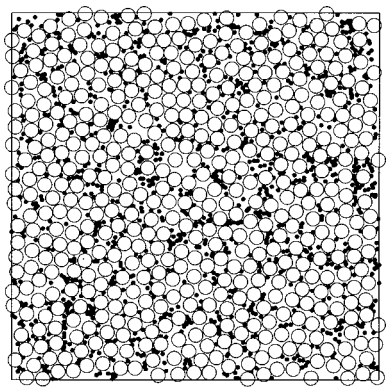

FIG. 4. Tethered RSA simulations. 1501 total particles; $\theta=0.66$, $\sigma=0.155$, $n_{S,\mathrm{bulk}}/n_{L,\mathrm{bulk}}=2$, $n_S/n_L=2$ (maintained number fraction), and $L/R_L=\infty$. Note that the smaller disks are displayed magnified for easier viewing.

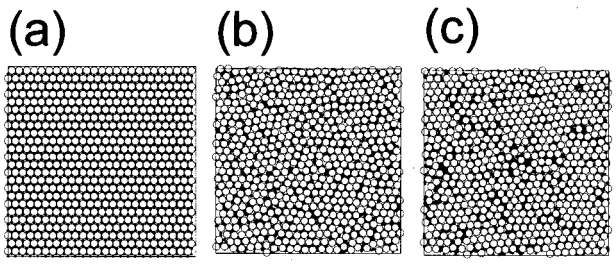

FIG. 5. Mechanical stability of an LS_2 lattice with $\sigma=0.155$ and $\theta=0.79$ after (a) zero, (b) 10 000, and (c) 1 000 000 diffusion cycles. Note that the smaller disks are displayed magnified for easier viewing.

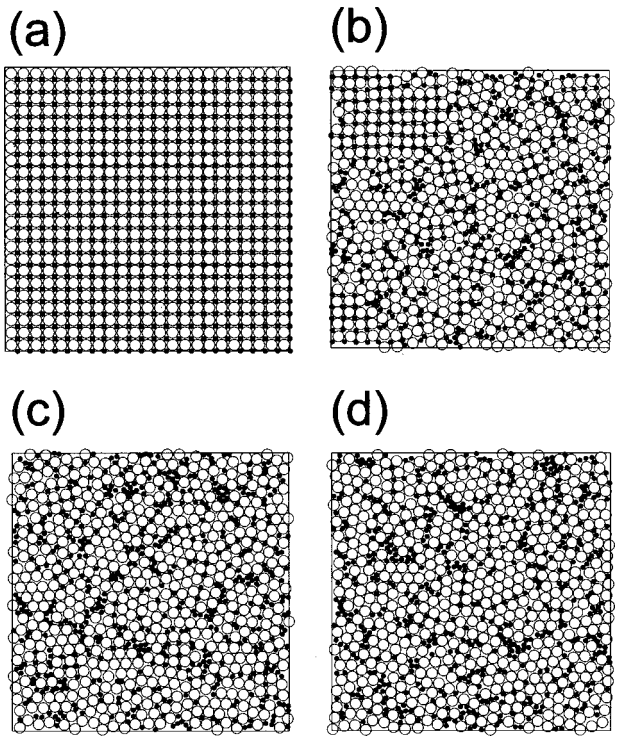

FIG. 6. Mechanical stability of an *LS* lattice with $\sigma=0.414$ and $\theta=0.78$ after (a) zero, (b) 500 000, (c) 1 000 000, and (d) 1 500 000 diffusion cycles.

calculations essentially rely on *free volume* entropy and ignore *configurational* entropy contributions to the free energy, it is not clear how applicable these calculations are towards determining thermodynamically stable phases in 2D. Despite the uncertain possibility of thermodynamically stable L_mS_n phases of hard disks in 2D at high density, the bidisperse disk monolayers clearly do not attain sufficiently high packing fractions with the appropriate ratio of large and small disks on the surface for order to occur. The RSA process does not provide kinetic access to the very high-density phases of bidisperse disks in 2D required for mechanical stability of the L_mS_n lattices, and the observed structures represent kinetically ''locked'' phases as a result of the ''kinetic bottleneck'' to ordering.

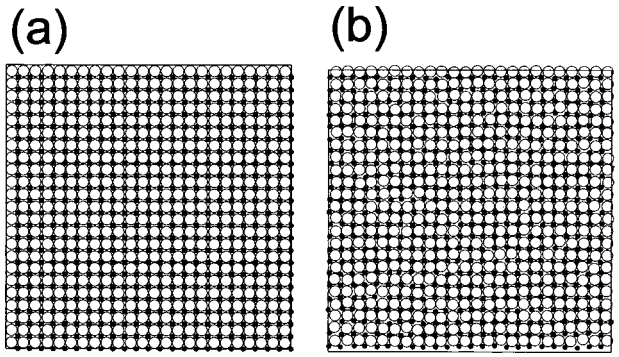

FIG. 7. Mechanical stability of an *LS* lattice with $\sigma=0.414$ and $\theta=0.81$ after (a) zero and (b) 1 250 000 diffusion cycles.

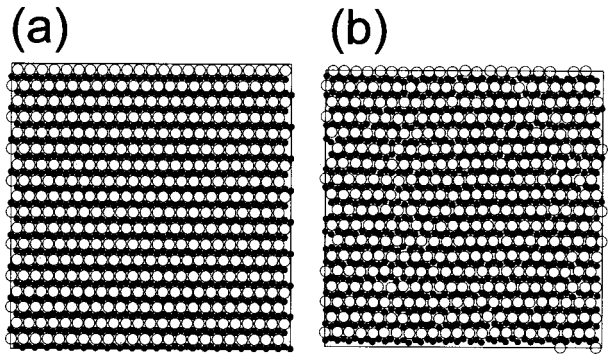

FIG. 8. Mechanical stability of an LS_2 lattice with $\sigma=0.53$ and $\theta=0.82$ after (a) zero and (b) 1 000 000 diffusion cycles.

The tethered RSA simulations presented here indicate that the bidisperse lattices of hard disks may not be the *thermodynamically* stable phases in 2D at high packing fractions. It is worthwhile to keep in mind that monodisperse disks [24], and polydisperse disks with a limited size distribution [25], readily organize into lattices during the tethered RSA process, and so one must cautiously approach the use of geometric packing calculations for determining stable L_mS_n phases in 2D. In two dimensions, the system entropy plays an important role in particle organization that is qualitatively different than 3D systems. Clearly, the experimental results of Kiely and coworkers [21] demonstrate that two-dimensional ordering of bidisperse sterically stabilized nanocrystals occurs. The hard disk potential is not expected

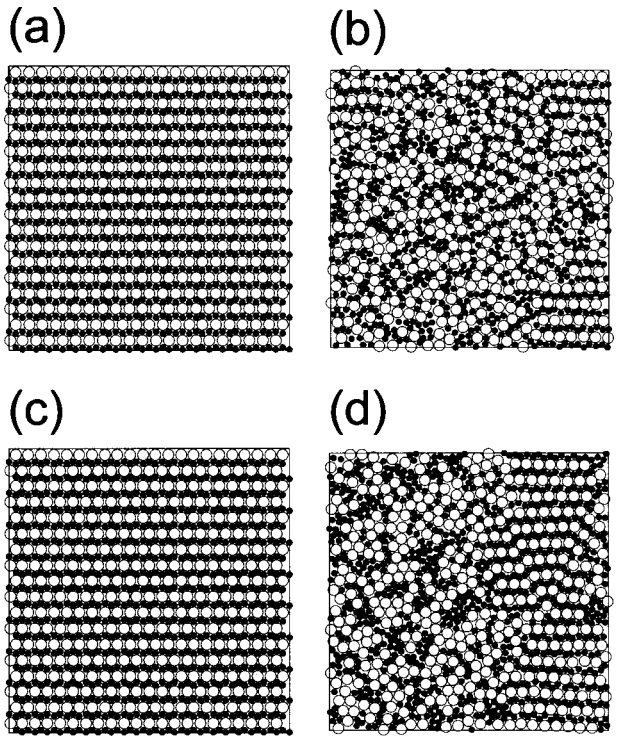

FIG. 9. Comparison of the mechanical stability of two LS_2 lattices with different starting surface coverage, with $\sigma=0.53$ and $\theta=0.74$ after (a) zero and (b) 30 000 diffusion cycles; and $\theta=0.78$ after (c) zero and (d) 4 500 000 diffusion cycles.

to be far from the actual interparticle potential for sterically stabilized nanocrystals [32]. As of now, however, we can only speculate that either the nature of the interparticle potential is significantly different from that of hard spheres, or the path to freezing of the bidisperse monolayers allows the ordered lattice to be formed. Equilibrium calculations of L_mS_n phases in 2D would be useful in determining the applicability of geometric packing calculations to real colloidal systems, as well as to determine the ordered phases worth targeting experimentally.

ACKNOWLEDGMENTS

The authors thank Harley Klein, Jeff Gray, and Emily Gray for valuable discussions about the tethered RSA procedure. B.A.K also thanks NSF and the Welch Foundation for partial financial support of this work.

[1] P. M. Chaikin and T. C. Lubensky, *Principles of Condensed Matter Physics*, 1st ed. (Cambridge University Press, Cambridge, 1995).
[2] B. J. Alder and T. E. Wainwright, J. Chem. Phys. **27**, 1208 (1957).
[3] J. D. Bernal, Nature (London) **183**, 141 (1959).
[4] P. Bartlett, R. H. Ottewill, and P. N. Pusey, Phys. Rev. Lett. **68**, 3801 (1992).
[5] M. D. Eldridge, P. A. Madden, and D. Frenkel, Nature (London) **365**, 35 (1993).
[6] E. Trizac, M. D. Eldridge, and P. A. Madden, Mol. Phys. **90**, 675 (1997).
[7] X. Cottin and P. A. Monson, J. Chem. Phys. **102**, 3354 (1995).
[8] N. Hunt, R. Jardine, and P. Bartlett, Phys. Rev. E **62**, 900 (2000).
[9] A. B. Schofield, Phys. Rev. E **64**, 051403 (2001).
[10] S. Hachisu and S. Yoshimura, in *Physics of Complex and Supermolecular Fluids*, edited by S. A. Safran and N. A. Clark (Wiley, New York, 1987), pp. 221–240.
[11] J. V. Sanders, Philos. Mag. A **42**, 705 (1980).
[12] M. J. Murray and J. V. Sanders, Philos. Mag. A **42**, 721 (1980).
[13] R. E. Peirls, Ann. Inst. Henri Poincaré **5**, 177 (1935).
[14] M. D. Mermin, Phys. Rev. **176**, 250 (1968).
[15] A. Jaster, Phys. Rev. E **59**, 2594 (1999).
[16] H. Weber, D. Marx, and K. Binder, Phys. Rev. B **51**, 14 636 (1995).
[17] J. M. Kosterlitz and D. J. Thouless, J. Phys. C **6**, 1181 (1973).
[18] B. I. Halperin and D. R. Nelson, Phys. Rev. Lett. **41**, 121 (1978).
[19] A. P. Young, Phys. Rev. B **19**, 1855 (1979).
[20] C. N. Likos and C. L. Henley, Philos. Mag. B **68**, 85 (1993).
[21] C. J. Kiely, J. Fink, M. Brust, D. Bethell, and D. J. Schiffrin, Nature (London) **396**, 444 (1998). C. J. Kiely, J. Fink, J. G. Zheng, M. Brust, D. Bethell, and D. J. Schiffrin, Adv. Mater. **12**, 640 (2000).
[22] J. Roth, R. Schilling, and H. R. Trebin, Phys. Rev. B **51**, 15 833 (1995).
[23] Nonetheless, metastable state stability of hard spheres in 3D has been recently studied. See, for example, P. Richard, L. Oger, J.-P. Troadec, and A. Gervois, Phys. Rev. E **60**, 4551 (1999).
[24] J. J. Gray, D. H. Klein, R. T. Bonnecaze, and B. A. Korgel, Phys. Rev. Lett. **85**, 4430 (2000).
[25] J. J. Gray, D. H. Klein, B. A. Korgel, and R. T. Bonnecaze, Langmuir **17**, 2317 (2001).
[26] J. Feder, J. Theor. Biol. **87**, 237 (1980).
[27] R. H. Swendsen, Phys. Rev. A **24**, 504 (1981).
[28] Despite our search in the literature for simulations of ordered L_mS_n lattices of hard spheres in 2D, we failed to find any. See, for example, W. M. Visscher and M. Bolsterli, Nature (London) **239**, 504 (1972); A. S. Nowick and S. R. Mader, IBM J. Res. Dev. **9**, 358 (1965).
[29] Recent simulations of symmetric binary Lennard-Jones mixtures in two dimensions revealed that ordered phases of bidisperse hard disks form under these conditions; M. J. Vlot and J. P. van der Eerden, J. Chem. Phys. **109**, 6043 (1998).
[30] M. P. Allen and D. J. Tildesley, *Computer Simulation of Liquids* (Oxford University Press, Oxford, 1987).
[31] J.-S. Wang and R. B. Pandey, Phys. Rev. Lett. **77**, 1773 (1996).
[32] B. A. Korgel and D. Fitzmaurice, Phys. Rev. B **59**, 14 191 (1999).